Earth **Surface**
Dynamics
Discussions
EGU

Short communication: Significance assessment of historical surfacic planform changes of mid-sized rivers: A Monte-Carlo based approach.

Timothée Jautzy[1], Pierre-Alexis Herrault[1], Valentin Chardon[1], Laurent Schmitt[1], and Gilles Rixhon[1,2]

[1]Laboratoire Image, Ville, Environnement (LIVE UMR 7362), Université de Strasbourg, CNRS, ENGEES, ZAEU LTER, 3 rue de l'Argonne, 67083 Strasbourg, France
[2]Laboratoire Image, Ville, Environnement (LIVE UMR 7362), ENGEES, CNRS, Université de Strasbourg, 1 quai Koch, 67070 Strasbourg, France

Correspondence: Timothée Jautzy (timothee.jautzy2@etu.unistra.fr)

Abstract.

Remote-sensed data in the fluvial context are extensively used to document historical planform changes. However, geometric and delineation errors inherently associated with these data can result in poor or even misleading interpretation of measured changes, especially (rates of) channel lateral migration. It is thus fundamental to take a spatially-variable (SV) error affecting

5   remote-sensed data into account. In the wake of recent key studies using this SV-error as a level of detection, we introduce a new framework to evaluate the significance of measured channel migration. Going beyond their linear metric (i.e. migration vectors between diachronic river centrelines), we assess this significance through the channel polygon method yielding a surfacic metric (i.e. quantification of eroded, deposited, or eroded/deposited surfaces).

Our study area is an active wandering mid-sized river: the lower Bruche, a ∼20 m wide sub-tributary of the Rhine in eastern

10 France. Within our four test sub-reaches, the active channel is digitised using diachronic orthophotos (1950; 1964) and the sub-reach specific SV-error affecting the data is interpolated with an Inverse Distance Weighting (IDW) technique. A main novelty of our approach consists then in running Monte-Carlo (MC) simulations to randomly translate active channels and propagate geometric and delineation errors according to the SV-error. This eventually leads to the production of a Surface of Detection (SoD), which allows evaluating the significance of measured surfacic changes. Putting the SoD into practice

15 in the lower Bruche shows that only 37% of the total surfacic measured changes are significant. Our results suggest that (i) orthophotos are affected by a significant SV-error, (ii) the latter strongly affects the significance of measured changes and (iii) the significance is strongly dependent on the magnitude of surfacic changes. Taking the SV-error into account is strongly recommended, regardless of the remote-sensed data used (orthophotos or aerial photos), especially in the case of mid-sized rivers (<30 m width) and/or low amplitude river planform changes (<1000 m²/yr). We finally insist on the transposability of

20 our approach as we use well-established tools (IDW, MC): this opens new perspectives in the fluvial context (e.g. multi-thread river channels) for robustly assessing surfacic changes.

1   Introduction

In the fluvial context, remote-sensed data opportunely provides spatial information on historical lateral dynamics of river channels (Bollati et al., 2014; Cadol et al., 2010; Comiti et al., 2011; Gurnell et al., 1994; Hajdukiewicz and Wyżga, 2019; Wesley Lauer et al., 2017). This is of crucial importance for e.g. creating a scientific framework transposable to sustainable management of hydrosystems, including river restoration (Biron et al., 2014; Piégay et al., 2005; Surian et al., 2009). Aerial photographs are thus commonly used to document and measure planform channel changes of at the most the last century, in a wide variety of fluvial settings. Requiring data coregistration and river bank digitisation, these planimetric studies generally result in the extraction of morphological metrics such as channel width (Gilvear, 2004; Werbylo et al., 2017; Winterbottom, 2000) or lateral migration (Hooke and Yorke, 2010; Janes et al., 2017; Mandarino et al., 2019; O'Connor et al., 2003) to characterise their evolution in time (e.g. rates of lateral migration).

However, two major sources of spatial uncertainties inherently question the robustness of these planimetric methods: the delineation error due to digitisation of river banks (Downward et al., 1994; Güneralp et al., 2014; Gurnell et al., 1994; Micheli and Kirchner, 2002; Werbylo et al., 2017) and the geometric error due to data coregistration (Gaeuman et al., 2005; Hughes et al., 2006; Liébault and Piégay, 2001; Payraudeau et al., 2010; Swanson et al., 2011). Whatever the scope of the study and the environmental context, these uncertainties needs to be assessed as accurately as possible (De Rose and Basher, 2011; Donovan et al., 2019; Mount and Louis, 2005; Mount et al., 2003). In that way, the Root Mean Square Error (RMSE) has been frequently used over the last decades to assess a uniform geometric error affecting coregistrated planimetric data (Table 1). Lea and Legleiter (2016) however demonstrated that the RMSE approach was too simplistic because coregistrated data are affected by spatially-variable (SV) geometric error. To test its impact on the quantification of lateral migration, the SV-error was used as a SV Level of Detection (LoD): it allowed detecting 33 % of statistically significant changes (migrations) instead of only 24 % with the RMSE/uniform error approach (Lea and Legleiter, 2016). The thorough review of Donovan et al. (2019) lately reached the same conclusion: they encouraged the generalisation of SV-error assessment and also notified the potential need (for instance in the case of complex planforms such as braided rivers) for testing SV-LoD on new metrics of lateral migration, such as surfacic ones.

Both Lea and Legleiter (2016) and Donovan et al. (2019) developed a LoD on a linear metric (Fig. 1a) implemented in the Planform Statistics Toolbox (Lauer, 2006), which reports fluvial planform changes as a linear adjustment. However, by conflating river banks onto an unique centreline (Fig. 1a), this last metric can oversimplify geomorphological changes. It is prone to fail detecting observed lateral adjustments when, for instance, channel widening or narrowing occurs without any significant lateral migration (Miller and Friedman, 2009; Rowland et al., 2016). This is all the more relevant for the less investigated mid-sized rivers (width<30 m; Table 1), which, despite their importance in terms of river geomorphological management (Marçal et al., 2017), might be more impacted by the aforementioned issues (e.g. delineation and geometric error).

This study aims at completing the generalisation of SV-error assessment methods in fluvial settings by testing its impact on the quantification of lateral migration, using a surfacic metric (Channel Polygon method; Fig. 1b). SV-error is assessed on two diachronic orthophotos of the lower Bruche (i.e., a mid-sized sub-tributary of the Rhine), by spatial interpolation (Lea and Legleiter, 2016) based on an independent set of ground control points (Hughes et al., 2006). A main novelty of our approach is

5 to run Monte-Carlo (MC) simulations (Metropolis and Ulam, 1949) to propagate the geometric error in measurements of eroded and/or deposited surfaces and produce a Surface of Detection (SoD) which allows detecting significant planform changes.

More specifically, this study tests three hypotheses in the fluvial context: (1) orthophotos are affected by a local significant SV-error; (2) SV-error significantly affects measurements of eroded and/or deposited surfaces; and (3) the higher the SV-error is, the less significant the measured changes are. This work also evaluates the effectiveness of MC simulations in measurements

10 of fluvially eroded and/or deposited surfaces and assessing their significance.

2 Study area

Located in the easternmost France (Alsace), the Bruche river is a western, mid-sized sub-tributary of the Rhine with a drainage area of about 730 km². The 80 km long river firstly drains the eastern flank of the Vosges Massif before debouching into the Upper Rhine Graben (Fig. 2a). Although highly impacted by human activities (levee/canal construction, channelisation,

15 artificial cut-offs), this alluvial river is known to have been laterally active over historical times (Maire, 1966; Payraudeau et al., 2010; Schmitt et al., 2007). This is especially true in its lowermost reach where it flows through the Strasbourg urban area (Fig. 2a), thereby raising important management issues (Payraudeau et al., 2008; Skupinski et al., 2009). Our test site is a 6 km long wandering reach located a few kilometres upstream of the Ill confluence: the river freely meanders within its Holocene floodplain and locally erodes Late Pleistocene terraces deposits of the lower Bruche about 2 km from its outlet as well (Fig.

20 2a; Maire, 1966). In this reach, the Bruche displays a 20 m wide mean active channel and a mean slope of 1‰. Elevation of the river banks decreases from 146 to 142 m above the sea level. The daily two-year (Q_2) and ten-year (Q_{10}) peak flow discharges amount to 71 m³/s and 126 m³/s, respectively (period 1965-2018). The specific stream power amounts to 30-35 W/m².

3 Methodology

3.1 Remote-sensed data

25 To measure eroded and/or deposited surfaces on our study area, two orthophotos from 1950 and 1964 were used. They were produced by the French National Geographic Institute (IGN) and the Laboratoire Image Ville Environnement (LIVE) of the University of Strasbourg; they have a spatial resolution of 50 and 20 cm, respectively. Both are projected in RGF93/CC48 CRS (EPSG: 3948), which is the most accurate projection in this area. Surveys were conducted during moderate-low water (09/13/50; 04/17/64).

30 Active channel is a widely used concept to objectively identify channel boundaries on aerial photographs. It basically refers to the unvegetated area (Liébault and Piégay, 2001; Liro, 2015; Mandarino et al., 2019; Surian et al., 2009; Winterbottom,

2000). Here, active channel boundaries have been digitised by a single user in QGIS at a 1/300 scale. To reliably assess the SV-error, we used a 2015 orthophoto as the base image; it was produced by the IGN with a resolution of 20 cm.

3.2 SV-error assessment

On both orthophotos (1950; 1964) of our study area, spatial variations of geometric error are assessed by an approach similar

5 to that used by Lea and Legleiter (2016). However, because we use orthophotos (which are already coregistered), we must rely on an independent set of GCPs, as suggested such by Hughes et al. (2006). We selected a total of 18 GCPs, including both hard (buildings, canal) and soft (pathways intersections, trees) edges (Fig. 3). After identification and manual plotting on the 2015 orthophoto, they are incorporated to both older orthophotos at a 1/200 computer-screen scale. The spatial distribution of GCPs in the study area is rather uniform, though hard edges are restricted to the northern sector (Fig. 3).

10 Local RMSE is then measured for each of the 18 GCPs, on both orthophotos. SV-error is calculated by interpolating local RMSE on our whole study area with an Inverse Distance Weighting (IDW) technique at the original spatial resolution (Fig. 4). IDW uses a linear combination of values at specific sampled points. It allocated weights proportionally to the proximity of the sampled points to estimate values of the unknown locations (Ikechukwu et al., 2017). We used the IDW interpolation method for two main reasons. First, Lea and Legleiter (2016) showed the necessity to use interpolation methods that do not reduce the

15 areal extent of relatively large error, i.e cubic or spline compared to linear or natural neighbour interpolation methods. Then, in a comparative study of spatial interpolation methods to produce Digital Elevation Model from a small set of points not spatially uniform, Tan and Xu (2014) showed IDW provided better results than Spline or Kriging. Because of the difficulties to select a high number of independent control points spatially uniform over time in old spatial data, we argue that it is a crucial point to consider.

20 ## 3.3 Sub-reaches and local specific geometric error (LSE)

To compare the implications of SV-error on lateral migration measurements, we focus on four distinct several hundred meters long sub-reaches (Fig. 2). They respectively are (1) an extending meander, (2) an almost straight (apparently inactive) sector, (3) two alternate meanders (the first one slightly extending) and (4) a long meander slightly extending at the downstream curvature.

25 The SV-error allows determining a local specific geometric error (LSE) affecting the four sub-reaches. LSEs are sub-reach-specific: (i) they are a mean error calculated for each sub-reach, (ii) they are uniform within each sub-reach and (iii) they spatially and temporally differ from one sub-reach to one another.

3.4 MC simulations

3.4.1 Channel boundaries simulation method

30 Monte Carlo (MC) simulations as statistical methods are generally used in cases where processes are random or when assumptions in the theoretical mathematics are badly known (Brown and Duh, 2004; Openshaw et al., 1991). Applying MC

simulations in this research context is a main novelty of this study. It results in two main advantages. Firstly, MC simulations are particularly well suited to our problem because of the difficulty to distinguish inherent and processing errors in the measured RMSE over the whole area. Secondly, they assume a spatial continuity and a relative spatial homogeneity of the error, which is consistent with resulting spatial patterns of errors observed after coregistrating or digitising process. MC are also rel-

5   atively easy to perform and applicable in very different cases. This could improve the generalisation of methods for calculating planform changes and spatially variable uncertainty in a fluvial context, as suggested by Donovan et al. (2019).

The approach used in this study followed the rules of boundary simulations (Burrough et al., 2015). As described in the previous section, LSEs were assigned to the channel boundaries for the two years in each sub-reach. Then, a normal distribution of error (d_n) was calculated by averaging the LSE of each node ($_n$) in each sub-reach and by calculating the standard deviation

10 ($_n$). Hence, at each run (1000 runs in total), a value of error in x ($e_x[i = 1, ..., 1000]$) and y ($e_y[i = 1, ..., 1000]$) was randomly extracted in order to shift each node from its original position (see equation 1 and 2). Furthermore, similarly to Podobnikar (2008), the shape of a particular channel is assumed to remain similar after simulation. Indeed, the simulation process of error must not alter the manual digitisation of the producer. Respecting that condition, it must exist a correlation between nodes within the simulation of one channel. The correlation coefficient (CORR) depends on correlation between generalisation of the

15 vector lines and/or the ratio between the absolute and the relative accuracy. To simplify this point, CORR was assumed equal to 1 for every node of the channel boundary so each of them were shifted to a similar distance in x and y (i.e. e_x and e_y) at a simulation run. From a similar way, the direction of errors in x and y, i.e. negative or positive, was randomly selected at each MC run and applied uniformly for every node of the river channel.

Last, as mentioned by Donovan et al. (2019), it is quite hard to distinguish errors inherent to coregistrating and digitising

20 process. For this reason, a digitising error (e_d) equal to 1 pixel was added as a reasonable constraint within the simulation process, considering the resolution of the orthophotos. This digitising error is assumed to be uniform over the entire area and does not fluctuate in different simulation runs.

The overall mathematical expression of the simulation process can be expressed as follows:

$$x_{changed} = x_{original} + (e_x \times CORR) + e_d \tag{1}$$

25

$$y_{changed} = y_{original} + (e_y \times CORR) + e_d \tag{2}$$

3.4.2   Lateral migration measurements

Lateral migration of the river channel between 1950 and 1964 is calculated through three standard surfacic morphological

30 metrics (erosion, deposition, both erosion/deposition) illustrated in figure 1b. Therefore, at each MC run, new values of metrics are derived for each sub-reach in order to estimate fluctuations induced by coregistrating and digitising errors.

3.4.3 Assessment of the statistical significance of the migration measurements

To determine if lateral migration measured in each sub-reach is significant or not, a virtual Surface of Detection (SoD) was estimated. The SoD refers to a virtual surface which allows us to distinguish significant measurements from the insignificant ones, for each sub-reach. It can be considered as the surfacic equivalent of the linear LoD introduced by Lea and Legleiter

5 (2016) and corresponds to the range of measured surfaces (erosion, deposition, erosion/deposition) through the MC simulations. Two types of SoD are used: (1) The raw-SoD is calculated by subtracting the very maximum measured value by the very minimum measured value and (2) the 95-SoD, calculated by subtracting the maximum measured value by the minimum value, inside the 95 % confidence interval. We finally considered that significant lateral migration measurements corresponds to the average measured values minus the SoD.

10 ## 4 Results

4.1 SV-error and LSEs

Fig. 5 displays the LSE calculated for each sub-reach and year, from interpolated SV-error (Fig. 4). Sub-reach 4 is respectively affected by the highest (1.32 m) and the lowest (0.61 m) LSE in 1950 and in 1964. These values corresponds to the range of LSEs reached by the four sub-reaches. Sub-reach 1, 2 and 3 have a similar LSE between 1950 and 1964, while the LSE for

15 sub-reach 4 is divided by two between 1950 and 1964. LSE decreases from about 1.2 to 0.6 m, from sub-reach 1 to sub-reach 3.

4.2 MC simulations

An example of variations in measurements of eroded surface through MC simulations are presented for sub-reach 1 in figure 6. The entirety of MC results are available in appendix A. A large majority of the measurements appears to be randomly varying

20 around and close to the mean value, inside the 95 % confidence interval. Note that few outliers sometimes largely extends the maximum range (raw-SoD) compared to the 95 % confidence interval (95-SoD). It is especially the case when very low values of measurements occurs. For instance, MC simulations for sub-reach 1 let appears three outliers with values ($2.9 \cdot 10^3 m^2$) corresponding to 56 % of the mean measured value ($5.2 \cdot 10^3 m^2$).

Mean surfacic changes inferred from MC simulations between 1950 and 1964 are presented in figure 7a. Whatever the

25 sub-reach, changes in eroded or deposited surfaces are much larger than those associated to erosion/deposition. The latter are either negligible (1 and 3) or not recorded (2 and 4). Sub-reaches 1 and 2 show the largest and lowest surfacic changes, respectively: $5.1 \cdot 10^3 m^2$ and $7.2 \cdot 10^3 m^2$ of eroded and deposited surfaces (sub-reach 1) vs $0.9 \cdot 10^3 m^2$ for both (sub-reach 2). Intermediate surfacic changes are reported in sub-reaches 3 and 4 where they range between $1.3 - 1.6 \cdot 10^3 m^2$ (deposition) and $3.1 - 4.2 \cdot 10^3 m^2$ (erosion). Note that, in these two last sub-reaches, changes in eroded surfaces are at least twice higher

30 than those in deposited surfaces. A coefficient of variation (CV), calculated as the ratio between 95-SoD and mean measured

changes (Fig. 7a), allows visualising the variability in measurements of surfacic changes through MC simulations. CV lower than 1 means that the mean surfacic change is greater than the 95-SoD, leading to the assumption that changes are significant.

4.3 Migration significance

The statistical significance of the measurements in surfacic changes is presented with both the raw-SoD and the 95-SoD (Fig.
5   7b). The total percentage of significant changes globally increases from 17 % using the raw-SoD to 37 % using the 95-SoD. Whilst this increase of significance with the 95-SoD is the highest for sub-reach 1 (from 48 % to 86 % for eroded surfaces; from 35 % to 90 % for deposited surfaces), we also observe the outbreak of significant changes in sub-reach 3 (from 24 % to 66 % for eroded surfaces; from 0 % to 25 % for deposited surfaces) as well as in sub-reach 4 (from 59 % to 75 % for eroded surfaces; from 0 % to 24 % for deposited surfaces; Fig. 7b). Regardless of the SoD used, the eroded/deposited surfaces appears to be
10   insignificant. Appliance of the 95-SoD let emerged respectively 2.6 and 0.5 % of apparently significant eroded and deposited surfaces in sub-reach 2. The relatively strong increase in measurements significance from raw-SoD to 95-SoD, common to any sub-reach, is explained by the presence of outliers (Fig. 6), largely extending the raw-SoD in almost any sub-reach (Appendix A).

5   Discussion and research perspectives

15   At the light of these new results, we first discuss the three hypotheses underlying this study. In a second step, we propose some methodological guidelines together with promising further implications of this study.

5.1   SV-error implications on surfacic planform changes significance

Our results validate the first hypothesis: they confirm that orthophotos are affected by a significant SV-error. Within our relatively small (~6 km²) and flat study area, we interpolate a SV-error ranging from 0.26 to 1.89 m while LSE values range from
20   0.61 to 1.32 m for the four sub-reaches. This emphasises the need to take the SV-error into account and, importantly, to assess it (Lea and Legleiter, 2016; Donovan et al., 2019), even if the characteristics of the studied reach may appear unproblematic at first glance. Moreover, as orthophotos are used in this study, we draw particular attention on the relevance of this statement in the case of studies using coregistrated aerial photographs for similar purposes (e.g., Cadol et al., 2010; Hooke and Yorke, 2010; Sanchis-Ibor et al., 2019).
25   Our results validate the second hypothesis too: the SV-error strongly affects significance of measured eroded and/or deposited surfaces. Whereas the most conservative raw-SoD reduces the significance of the measured changes to only 17 %, the latter amounts to 37 % with the less conservative 95-SoD. Although this last value may appear low, it falls into the same range as the value (33 %) proposed by Lea and Legleiter (2016), who interestingly studied channels of similar width (~15 m). On threefold larger river systems (widths ~45 m), Donovan et al. (2019) found a total of 62 % of significant migration vectors
30   (Table 1). Corroborating these authors outcomes, our study surely demonstrates the need for distinguishing between significant and unsignificant changes, whatever the size of the fluvial system considered.

Our results partly refute the third hypothesis: the significance of measured changes does not only depend on SV-error magnitude. Indeed, the first sub-reach simultaneously displays the largest amount of significant changes in eroded and deposited surfaces (i.e. 86-90 % with the 95-SoD) and high LSEs (1.15 m for 1950; 1.20 m for 1964). On the other hand, the third sub-reach, though characterised by low LSEs (0.65 m on both orthophotos), does not exhibit any significant change for the very

5 low amount of eroded/deposited surfaces. Based on these both observations, we can suggest instead that the significance of measured planform changes may primarily depend on the magnitude of changes. A corollary is that the lower the measured changes are, the more the SV-error should be taken into account. As for the magnitude of planform changes, the annual rates in the lower Bruche amounting to ∼350 m²/yr (according to the eroded surfaces in sub-reach 1) contrast with those reported by Hooke and Yorke (2010) in a similar context (i.e. one order of magnitude more for the 15 m wide River Dane in the UK; Table

10 1). In those kind of settings, leaving aside the assessment of the SV-error, such as Hooke and Yorke (2010) did, might be more acceptable, provided that the magnitude of changes largely exceeds a certain threshold (e.g. 1000 m²/yr, though this value has to be better defined by further research).

5.2 Methodological guidelines and potential applications

In order to improve the generalisation of tools documenting fluvial planform changes and facilitate the implementation of

15 our new methodological framework, we can summarise the complete workflow as follows (see Fig. 8 for more details): (1) interpolate the SV-error on the study area (as recommended in Lea and Legleiter, 2016), (2) compute the LSEs affecting each sub-reach, (3) assess the SoDs affecting sub-reaches and (4) assess the significance of the measured surfacic planform changes. The key step (3) is achieved thanks to MC simulations (Fig. 8), which is well-known for its simplicity, reliability and transposability (Brown and Duh, 2004; Openshaw et al., 1991). Simulations outputs allow assessing both the raw and 95-SoDs

20 (Fig. 8).

We suggest a few practical recommendations when applying our methodological framework. If orthophotos are employed, we strongly advice using an independent set of GCPs for coregistration and bearing in mind that orthophotos are affected by a significant SV-error (see 5.1). As for GCPs, their amount must be high enough and their distribution over the entire study area as homogeneous as possible. As pointed out by Hughes et al. (2006), a location of these GCPs close to the river system is highly

25 beneficial. As for the SoD, we recommend using the 95-SoD as it refers to the most probable results and greatly improve the significance of the results. Nevertheless, the conservative raw-SoD might also be considered as it refers to situations which are (very) rare but possible. In this respect, the few outliers (Fig. 6) should be treated in an empirical manner by determining if they match geomorphologically plausible situations. This could be achieved for instance by visualising the two randomly translated overlaid river channels. More generally, when studying historical lateral migration of mid-sized rivers (<30 m) and/or low

30 magnitude changes (<1000 m²/y) with the Channel Polygon method, we suggest a systematical assessment of both SV-error and SoD as a majority of measured changes might be insignificant (see 4.3).

This study, though focusing on short sub-reaches of a mid-sized (∼20 m), meandering (single-thread) channel using specific remote-sensed data over a short timescale (ancient orthophotos), has a strong potential of transposability. Firstly, we assume that our methodological framework could be applied to any fluvial system, regardless its size. Secondly, we likewise argue
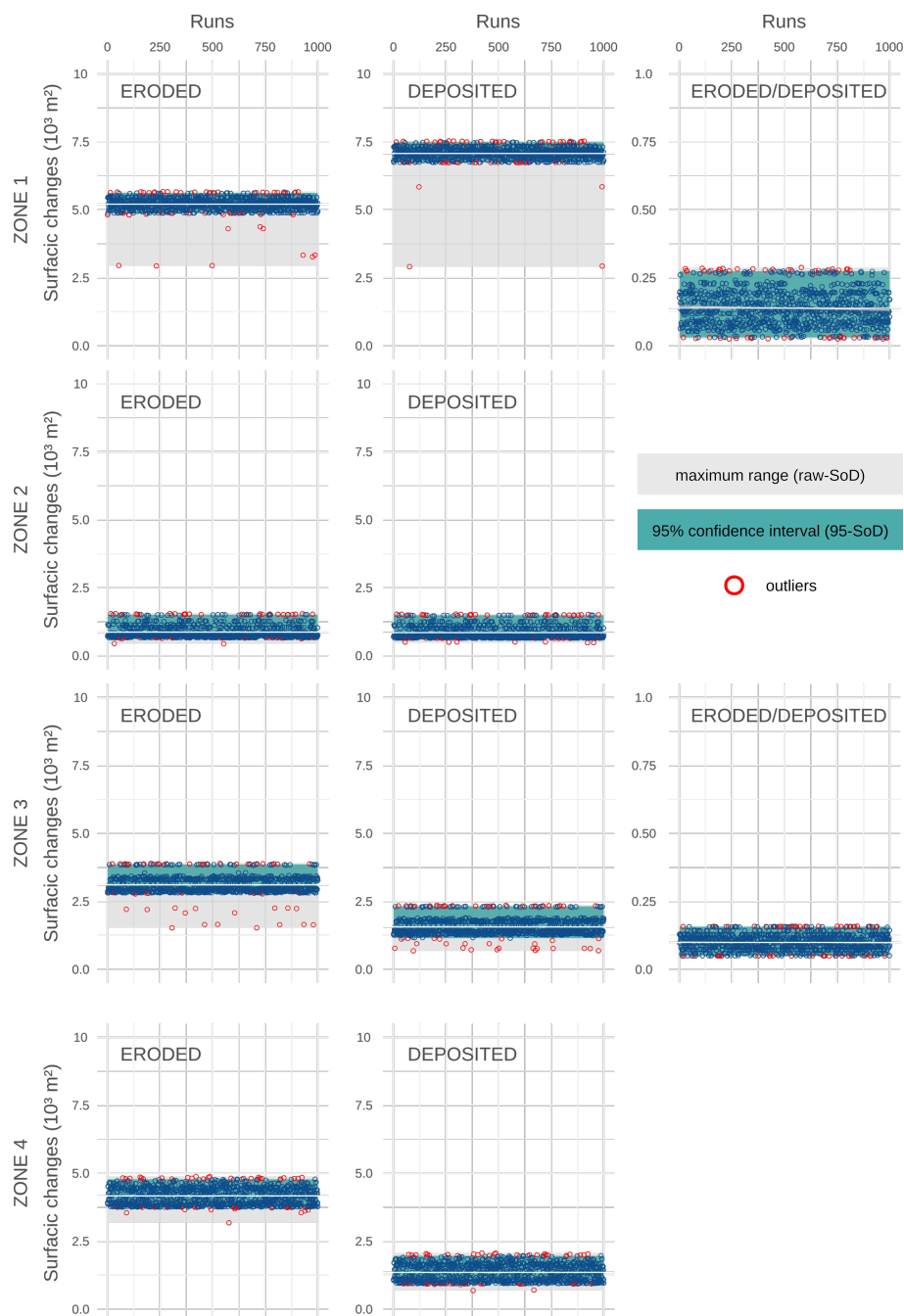
that it could be relatively easily extended onto an entire river reach by increasing the sub-reach database and/or onto a longer temporal scale by increasing the historical river channel database (Fig. 8). As for the latter, other remote-sensed data, such as coregistrated aerial photographs and satellite imagery, or traditional planimetric data (maps) can be easily integrated as well. Thirdly, transposing this framework to other channel patterns, in particular multi-thread river systems (e.g., Rowland et al.,

5 2016), represents a promising future perspective. By contrast to the Centreline approach (e.g., Lea and Legleiter, 2016), the Channel Polygon method would actually suit the study of lateral mobility of braided channels, with a robust assessment of the SV-error. Unlike this present study where planimetric changes associated to erosion/deposition are negligible, we might expect a much higher proportion of these changes in this kind of dynamic fluvial settings.

We conclude by stating that this study offers promising research perspectives. Firstly, a key outcome is the ability of MC

10 simulations to actually detect low-magnitude planform changes in mid-sized river channels. This positive achievement thus overcomes the main difficulty related to the use of classic planimetric methods in such settings (Piégay et al., 2005), as recently highlighted by Wesley Lauer et al. (2017), who failed detecting noticeable changes in mid-sized active channels (width<25 m). Secondly, as for river restoration, our methodological framework should help constructing robust scenarios of future river management, especially those based on past planform changes (e.g., Marçal et al., 2017). Thirdly, significance assessment

15 of planform changes can strengthen the studies using surfaces of active channel as input for sediment budgeting (Wheaton et al., 2009). Finally, whilst this study, together with Lea and Legleiter (2016) and Donovan et al. (2019), contributes drawing a specific attention to assess the SV-error and, more globally, uncertainties in planimetric studies in a wide range of fluvial settings, the proposed propagation of geometric error via MC simulations could be extended to other geomorphological contexts where surface extraction from remote-sensed data is involved.

20 *Author contributions.* All authors contributed to the conception of this study and manuscript writing. TJ wrote most of the manuscript, produced the initial data and figures; PAH developed the code and performed Monte-Carlo simulations; VC contributed to result interpretation; LS and GR provided a complete review of the manuscript; GR supervised the text harmonisation.

Competing interests. The authors declare that they have no conflict of interest.

Appendix A: Monte-Carlo simulation results for every sub-reach.

Earth **Surface**
Dynamics
Discussions

Open Access

EGU

References

Biron, P. M., Buffin-Bélanger, T., Larocque, M., Choné, G., Cloutier, C.-A., Ouellet, M.-A., Demers, S., Olsen, T., Desjarlais, C., and Eyquem, J.: Freedom Space for Rivers: A Sustainable Management Approach to Enhance River Resilience, Environmental Management, 54, 1056–1073, https://doi.org/10.1007/s00267-014-0366-z, 2014.

5 Bollati, I., Pellegrini, L., Rinaldi, M., Duci, G., and Pelfini, M.: Reach-scale morphological adjustments and stages of channel evolution: The case of the Trebbia River (northern Italy), Geomorphology, 221, 176–186, https://doi.org/10.1016/j.geomorph.2014.06.007, 2014.

Brown, D. G. and Duh, J.-D.: Spatial simulation for translating from land use to land cover, International Journal of Geographical Information Science, 18, 35–60, https://doi.org/10.1080/13658810310001620906, 2004.

Burrough, P. A., McDonnell, R., McDonnell, R. A., and Lloyd, C. D.: Principles of geographical information systems, Oxford university
10 press, 2015.

Cadol, D., Rathburn, S. L., and Cooper, D. J.: Aerial photographic analysis of channel narrowing and vegetation expansion in Canyon De Chelly National Monument, Arizona, USA, 1935-2004, River Research and Applications, pp. n/a–n/a, https://doi.org/10.1002/rra.1399, 2010.

Comiti, F., Da Canal, M., Surian, N., Mao, L., Picco, L., and Lenzi, M.: Channel adjustments and vegetation cover dynamics in a large gravel
15 bed river over the last 200years, Geomorphology, 125, 147–159, https://doi.org/10.1016/j.geomorph.2010.09.011, 2011.

De Rose, R. C. and Basher, L. R.: Measurement of river bank and cliff erosion from sequential LIDAR and historical aerial photography, Geomorphology, 126, 132–147, https://doi.org/10.1016/j.geomorph.2010.10.037, 2011.

Donovan, M., Miller, A., Baker, M., and Gellis, A.: Sediment contributions from floodplains and legacy sediments to Piedmont streams of Baltimore County, Maryland, Geomorphology, 235, 88–105, https://doi.org/10.1016/j.geomorph.2015.01.025, https://linkinghub.elsevier.
20 com/retrieve/pii/S0169555X15000458, 2015.

Donovan, M., Belmont, P., Notebaert, B., Coombs, T., Larson, P., and Souffront, M.: Accounting for uncertainty in remotely-sensed measurements of river planform change, Earth-Science Reviews, 193, 220–236, https://doi.org/10.1016/j.earscirev.2019.04.009, 2019.

Downward, S., Gurnell, A., and Brookes, A.: A methodology for quantifying river channel planform change using GIS, IAHS Publications-Series of Proceedings and Reports-Intern Assoc Hydrological Sciences, 224, 449–456, 1994.

25 Gaeuman, D., Symanzik, J., and Schmidt, J. C.: A Map Overlay Error Model Based on Boundary Geometry, Geographical Analysis, 37, 350–369, https://doi.org/10.1111/j.1538-4632.2005.00585.x, 2005.

Gilvear, D. J.: Patterns of channel adjustment to impoundment of the upper River Spey, Scotland(1942–2000), River Research and Applications, 20, 151–165, https://doi.org/10.1002/rra.741, 2004.

Gurnell, A. M., Downward, S. R., and Jones, R.: Channel planform change on the river dee meanders, 1876–1992, Regulated Rivers: Research
30 & Management, 9, 187–204, https://doi.org/10.1002/rrr.3450090402, 1994.

Güneralp, , Filippi, A. M., and Hales, B.: Influence of river channel morphology and bank characteristics on water surface boundary delineation using high-resolution passive remote sensing and template matching: river water delineation using remote sensing and template matching., Earth Surface Processes and Landforms, 39, 977–986, https://doi.org/10.1002/esp.3560, 2014.

Hajdukiewicz, H. and Wyżga, B.: Aerial photo-based analysis of the hydromorphological changes of a mountain river
35 over the last six decades: The Czarny Dunajec, Polish Carpathians, Science of The Total Environment, 648, 1598–1613, https://doi.org/10.1016/j.scitotenv.2018.08.234, 2019.

Earth Surface
Dynamics
Discussions

EGU

Hooke, J. M. and Yorke, L.: Rates, distributions and mechanisms of change in meander morphology over decadal timescales, River Dane, UK, Earth Surface Processes and Landforms, 35, 1601–1614, https://doi.org/10.1002/esp.2079, 2010.

Hughes, M. L., McDowell, P. F., and Marcus, W. A.: Accuracy assessment of georectified aerial photographs: implications for measuring lateral channel movement in a GIS, Geomorphology, 74, 1–16, 2006.

5 Ikechukwu, M. N., Ebinne, E., Idorenyin, U., and Raphael, N. I.: Accuracy Assessment and Comparative Analysis of IDW, Spline and Kriging in Spatial Interpolation of Landform (Topography): An Experimental Study, Journal of Geographic Information System, 09, 354–371, https://doi.org/10.4236/jgis.2017.93022, 2017.

Janes, V. J. J., Nicholas, A. P., Collins, A. L., and Quine, T. A.: Analysis of fundamental physical factors influencing channel bank erosion: results for contrasting catchments in England and Wales, Environmental Earth Sciences, 76, 307, https://doi.org/10.1007/s12665-017-6593-x, 2017.

10 Lauer, J. W. and Parker, G.: Net local removal of floodplain sediment by river meander migration, Geomorphology, 96, 123–149, https://doi.org/10.1016/j.geomorph.2007.08.003, 2008.

Lauer, W.: NCED Stream Restoration Toolbox-Channel Planform Statistics And ArcMap Project, National Center for Earth-Surface Dynamics (NCED), 2006.

15 Lea, D. M. and Legleiter, C. J.: Refining measurements of lateral channel movement from image time series by quantifying spatial variations in registration error, Geomorphology, 258, 11–20, https://doi.org/10.1016/j.geomorph.2016.01.009, 2016.

Legleiter, C. J.: Downstream Effects of Recent Reservoir Development on the Morphodynamics of a Meandering Channel: Savery Creek, Wyoming, USA, River Research and Applications, 31, 1328–1343, https://doi.org/10.1002/rra.2824, 2015.

Liro, M.: Estimation of the impact of the aerialphoto scale and the measurement scale on the error in digitization of a river bank, Zeitschrift
20 für Geomorphologie, 59, 443–453, https://doi.org/10.1127/zfg/2014/0164, 2015.

Liébault, F. and Piégay, H.: Assessment of channel changes due to long-term bedload supply decrease, Roubion River, France, Geomorphology, 36, 167–186, https://doi.org/10.1016/S0169-555X(00)00044-1, 2001.

Lovric, N. and Tosic, R.: Assessment of Bank Erosion, Accretion and Channel Shifting Using Remote Sensing and GIS: Case Study – Lower Course of the Bosna River, Quaestiones Geographicae, 35, 81–92, https://doi.org/10.1515/quageo-2016-0008, 2016.

25 Maire, G.: La Basse-Bruche : cône de piedmont et dynamique actuelle, Ph.D. thesis, Université de Strasbourg, Faculté de géographie et d'aménagement, 1966.

Mandarino, A., Maerker, M., and Firpo, M.: Channel planform changes along the Scrivia River floodplain reach in northwest Italy from 1878 to 2016, Quaternary Research, 91, 620–637, https://doi.org/10.1017/qua.2018.67, 2019.

Marçal, M., Brierley, G., and Lima, R.: Using geomorphic understanding of catchment-scale process relationships to support the management
30 of river futures: Macaé Basin, Brazil, Applied Geography, 84, 23–41, https://doi.org/10.1016/j.apgeog.2017.04.008, 2017.

Metropolis, N. and Ulam, S.: The Monte Carlo Method, Journal of the American Statistical Association, 44, 335–341, https://doi.org/10.1080/01621459.1949.10483310, 1949.

Micheli, E. R. and Kirchner, J. W.: Effects of wet meadow riparian vegetation on streambank erosion. 2. Measurements of vegetated bank strength and consequences for failure mechanics, Earth Surface Processes and Landforms, 27, 687–697, https://doi.org/10.1002/esp.340,
35 2002.

Miller, J. R. and Friedman, J. M.: Influence of flow variability on floodplain formation and destruction, Little Missouri River, North Dakota, Geological Society of America Bulletin, 121, 752–759, https://doi.org/10.1130/B26355.1, 2009.

Morais, E. S., Rocha, P. C., and Hooke, J.: Spatiotemporal variations in channel changes caused by cumulative factors in a meandering river: The lower Peixe River, Brazil, Geomorphology, 273, 348–360, https://doi.org/10.1016/j.geomorph.2016.07.026, 2016.

Mount, N. and Louis, J.: Estimation and propagation of error in measurements of river channel movement from aerial imagery, Earth Surface Processes and Landforms, 30, 635–643, https://doi.org/10.1002/esp.1172, 2005.

5 Mount, N., Louis, J., Teeuw, R., Zukowskyj, P., and Stott, T.: Estimation of error in bankfull width comparisons from temporally sequenced raw and corrected aerial photographs, Geomorphology, 56, 65–77, https://doi.org/10.1016/S0169-555X(03)00046-1, https://linkinghub.elsevier.com/retrieve/pii/S0169555X03000461, 2003.

O'Connor, J. E., Jones, M. A., and Haluska, T. L.: Flood plain and channel dynamics of the Quinault and Queets Rivers, Washington, USA, Geomorphology, 51, 31–59, https://doi.org/10.1016/S0169-555X(02)00324-0, 2003.

10 Openshaw, S., Charlton, M., and Carver, S.: Error propagation: a Monte Carlo simulation, Handling geographical information, pp. 78–101, 1991.

Payraudeau, S., Glatron, S., Rozan, A., Eleuterio, J., Auzet, A.-V., Weber, C., and Liébault, F.: Inondation en espace péri-urbain: convoquer un éventail de disciplines pour analyser l'aléa et la vulnérabilité de la basse-Bruche (Alsace), in: actes du colloque «Vulnérabilités sociétales, risques et environnement. Comprendre et évaluer», Université Toulouse–le Mirail, vol. 14, p. 15, 2008.

15 Payraudeau, S., Galliot, N., Liébault, F., and Auzet, A.-V.: Incertitudes associées aux données géographiques pour la quantification des vitesses de migration des méandres-Application à la vallée de la Bruche, Revue Internationale de Géomatique, 20, 221–243, 2010.

Piégay, H., Darby, S. E., Mosselman, E., and Surian, N.: A review of techniques available for delimiting the erodible river corridor: a sustainable approach to managing bank erosion, River Research and Applications, 21, 773–789, https://doi.org/10.1002/rra.881, 2005.

Podobnikar, T.: Simulation and Representation of the Positional Errors of Boundary and Interior Regions in Maps, in: Geospatial Vision,
20 edited by Moore, A. and Drecki, I., pp. 141–169, Springer Berlin Heidelberg, Berlin, Heidelberg, https://doi.org/10.1007/978-3-540-70970-1_7, 2008.

Rhoades, E. L., O'Neal, M. A., and Pizzuto, J. E.: Quantifying bank erosion on the South River from 1937 to 2005, and its importance in assessing Hg contamination, Applied Geography, 29, 125–134, https://doi.org/10.1016/j.apgeog.2008.08.005, 2009.

Rowland, J. C., Shelef, E., Pope, P. A., Muss, J., Gangodagamage, C., Brumby, S. P., and Wilson, C. J.: A morphology independent method-
25 ology for quantifying planview river change and characteristics from remotely sensed imagery, Remote Sensing of Environment, 184, 212–228, https://doi.org/10.1016/j.rse.2016.07.005, 2016.

Sanchis-Ibor, C., Segura-Beltrán, F., and Navarro-Gómez, A.: Channel forms and vegetation adjustment to damming in a Mediterranean gravel-bed river (Serpis River, Spain): Channel and vegetation adjustment to damming in a gravel bed river, River Research and Applications, 35, 37–47, https://doi.org/10.1002/rra.3381, 2019.

30 Schmitt, L., Maire, G., Nobelis, P., and Humbert, J.: Quantitative morphodynamic typology of rivers: a methodological study based on the French Upper Rhine basin, Earth Surface Processes and Landforms, 32, 1726–1746, https://doi.org/10.1002/esp.1596, 2007.

Schook, D. M., Rathburn, S. L., Friedman, J. M., and Wolf, J. M.: A 184-year record of river meander migration from tree rings, aerial imagery, and cross sections, Geomorphology, 293, 227–239, https://doi.org/10.1016/j.geomorph.2017.06.001, 2017.

Skupinski, G., BinhTran, D., and Weber, C.: Les images satellites Spot multi-dates et la métrique spatiale dans l'étude du changement urbain
35 et suburbain – Le cas de la basse vallée de la Bruche (Bas-Rhin, France), Cybergeo, https://doi.org/10.4000/cybergeo.21995, 2009.

Surian, N., Mao, L., Giacomin, M., and Ziliani, L.: Morphological effects of different channel-forming discharges in a gravel-bed river, Earth Surface Processes and Landforms, 34, 1093–1107, https://doi.org/10.1002/esp.1798, 2009.
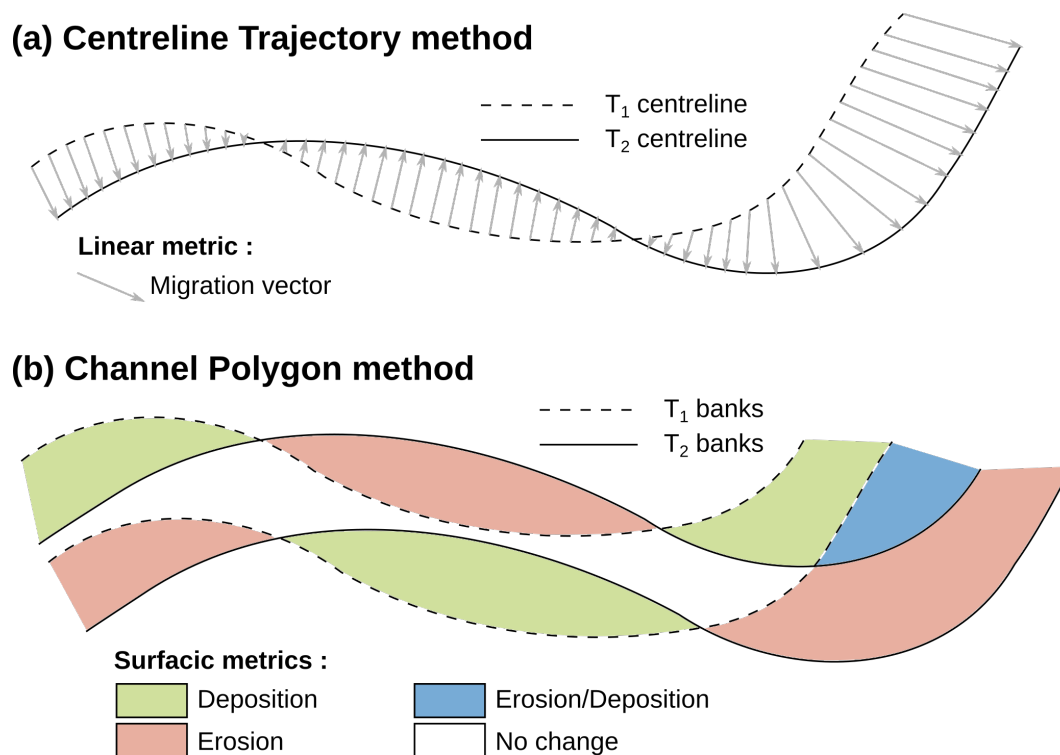
Earth **Surface**
Dynamics
Discussions

EGU

Swanson, B. J., Meyer, G. A., and Coonrod, J. E.: Historical channel narrowing along the Rio Grande near Albuquerque, New Mexico in response to peak discharge reductions and engineering: magnitude and uncertainty of change from air photo measurements, Earth Surface Processes and Landforms, 36, 885–900, https://doi.org/10.1002/esp.2119, 2011.

Tan, Q. and Xu, X.: Comparative Analysis of Spatial Interpolation Methods: an Experimental Study, Sensors & Transducers, 165, 9, 2014.

5 Werbylo, K. L., Farnsworth, J. M., Baasch, D. M., and Farrell, P. D.: Investigating the accuracy of photointerpreted unvegetated channel widths in a braided river system: a Platte River case study, Geomorphology, 278, 163–170, https://doi.org/10.1016/j.geomorph.2016.11.003, 2017.

Wesley Lauer, J., Echterling, C., Lenhart, C., Belmont, P., and Rausch, R.: Air-photo based change in channel width in the Minnesota River basin: Modes of adjustment and implications for sediment budget, Geomorphology, 297, 170–184,
10 https://doi.org/10.1016/j.geomorph.2017.09.005, 2017.

Wheaton, J. M., Brasington, J., Darby, S. E., and Sear, D. A.: Accounting for uncertainty in DEMs from repeat topographic surveys: improved sediment budgets, Earth Surface Processes and Landforms, pp. n/a–n/a, https://doi.org/10.1002/esp.1886, 2009.

Winterbottom, S. J.: Medium and short-term channel planform changes on the Rivers Tay and Tummel, Scotland, Geomorphology, 34, 195–208, https://doi.org/10.1016/S0169-555X(00)00007-6, 2000.
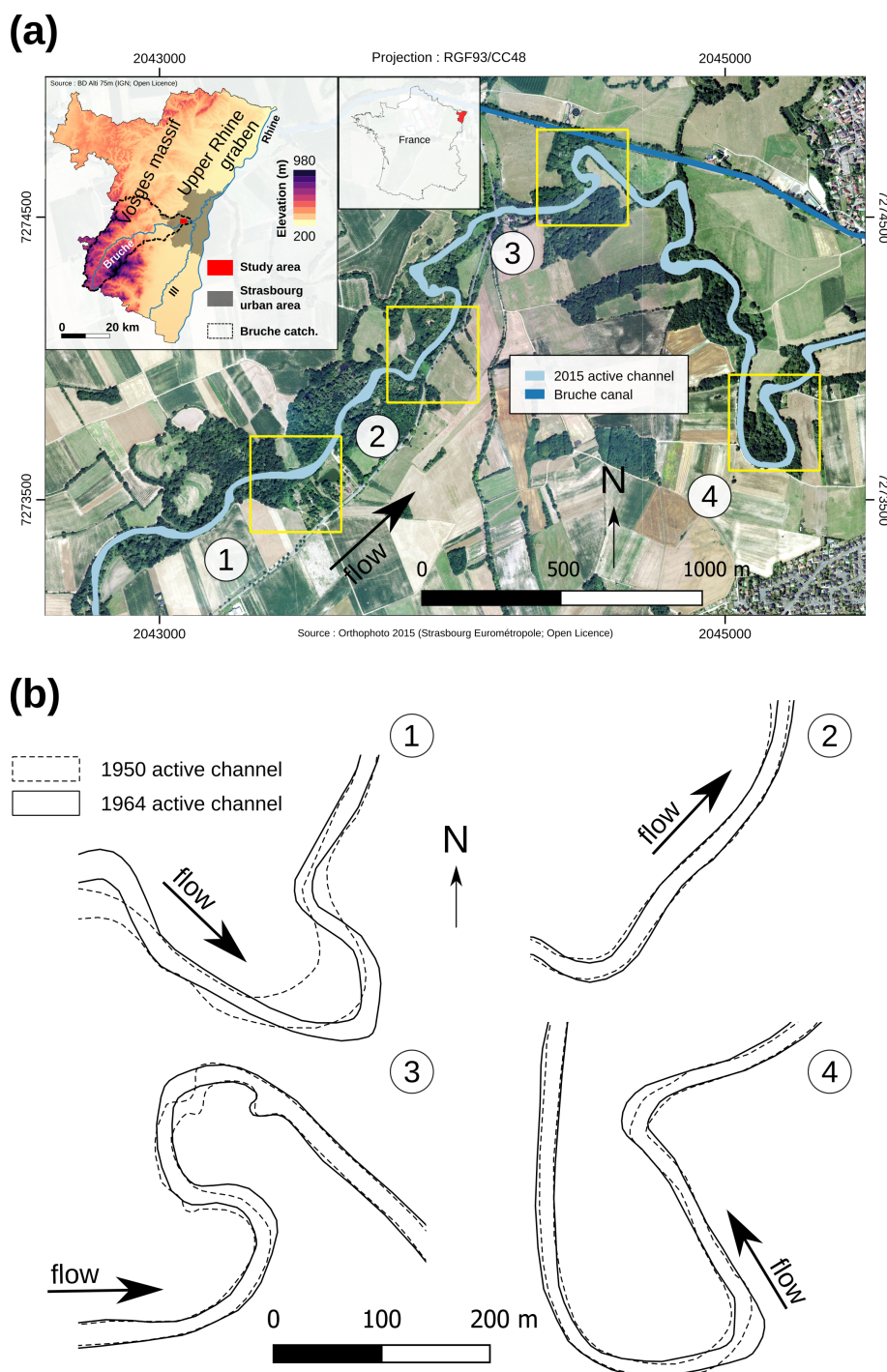
Table 1. Literature review of recent studies quantifying channel lateral migration using P: Channel Polygon method and/or T: Centreline Trajectory method. X: error not assessed. U: use of an uniform error. SV: use of a spatially-variable error. The table is sorted by the mean width of the channel(s) studied.

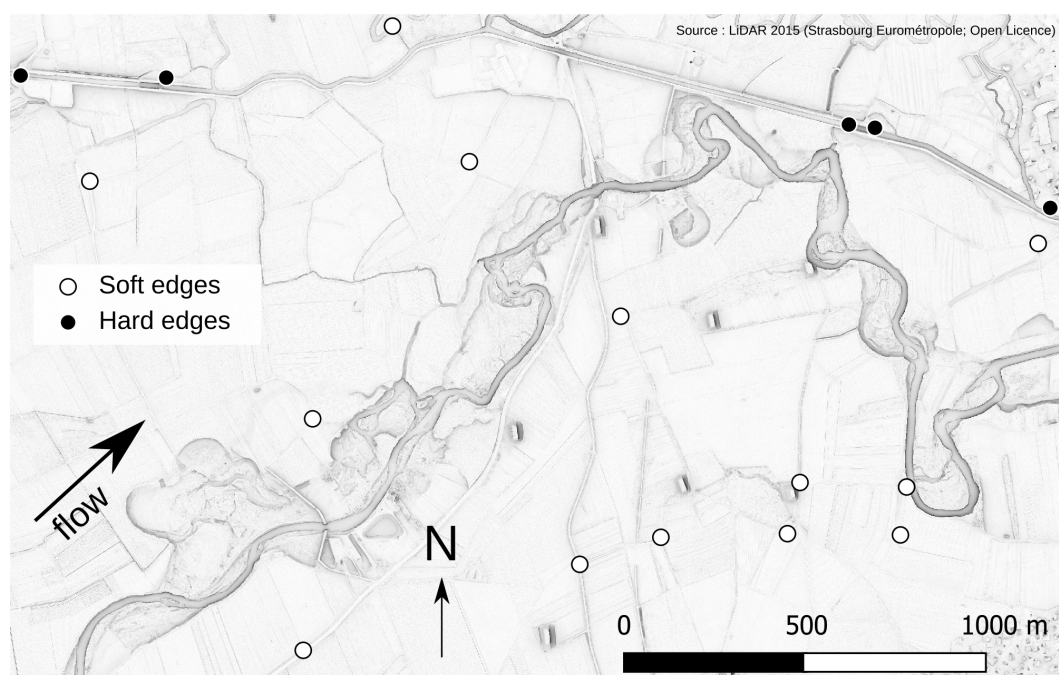| Authors (year)	Lateral migration metric	Delineation error (m)	Geometric error (m)	Channel width (m)	Erosion order of magnitude (m²/yr)
Donovan et al. (2015)	P/T	x	U: 1.0	1-12	/
Hooke and Yorke (2010)	P	U: 1.0	x	15	3230
Legleiter (2015)	P/T	x	U: 0.8-1.8	10-20	/
Lea and Legleiter (2016)	T	U: 2.0	SV: 0-5	15	/
this study	**P**	**U: 0.5**	**SV: 0.3-1.9**	**20**	**360**
Sanchis-Ibor et al. (2019)	P	x	U: 1.5	7-40	/
Gurnell et al. (1994)	P	U: 2.0	U: 1.4-4.5	30	500
Rhoades et al. (2009)	P	x	U: <1.0	30	1375
Janes et al. (2017)	P	x	U: 3.5	35	/
Donovan et al. (2019)	T	U: 1.4	SV: 0-10	45	/
Schook et al. (2017)	T	x	U: <1.6	50	/
Morais et al. (2016)	P	x	U: 0.9-3.6	30-80	760
Wesley Lauer et al. (2017)	T	x	U: 2.3	11.5-107.3	/
Lauer and Parker (2008)	T	x	U: 2.3-6.6	150;50;50;15	/
Lovric and Tosic (2016)	P	x	x	130	151 000
O'Connor et al. (2003)	P/T	x	x	90-240	/

Figure 1. Illustration of the lateral migration metric used (a) by Lea and Legleiter (2016) and Donovan et al. (2019) and (b) in this study.
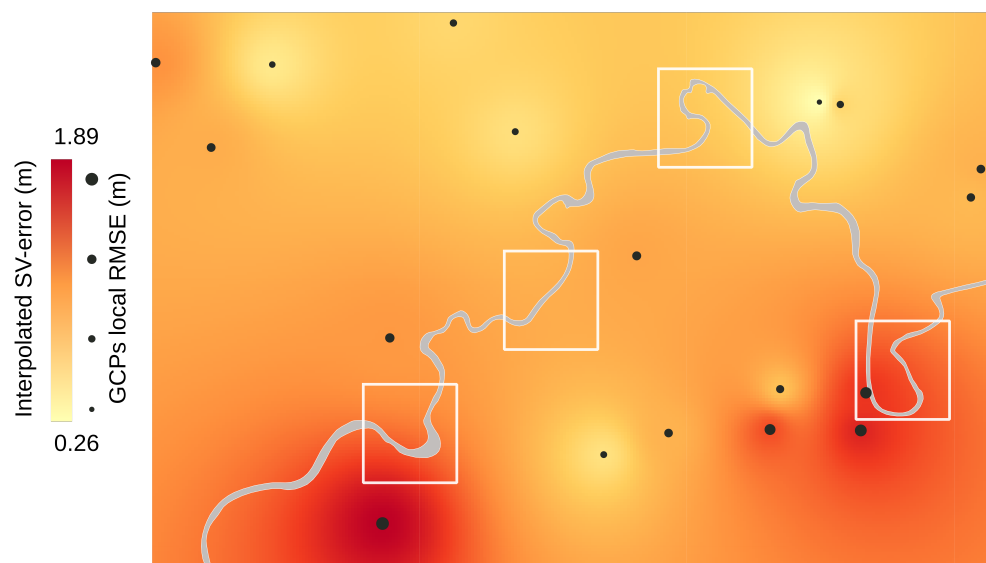
Figure 2. (a) Study area. Localisation of the four sub-reaches in the lowermost Bruche course. (b) Planimetric evolution of each sub-reach from 1950 to 1964 based on the two orthophotos.
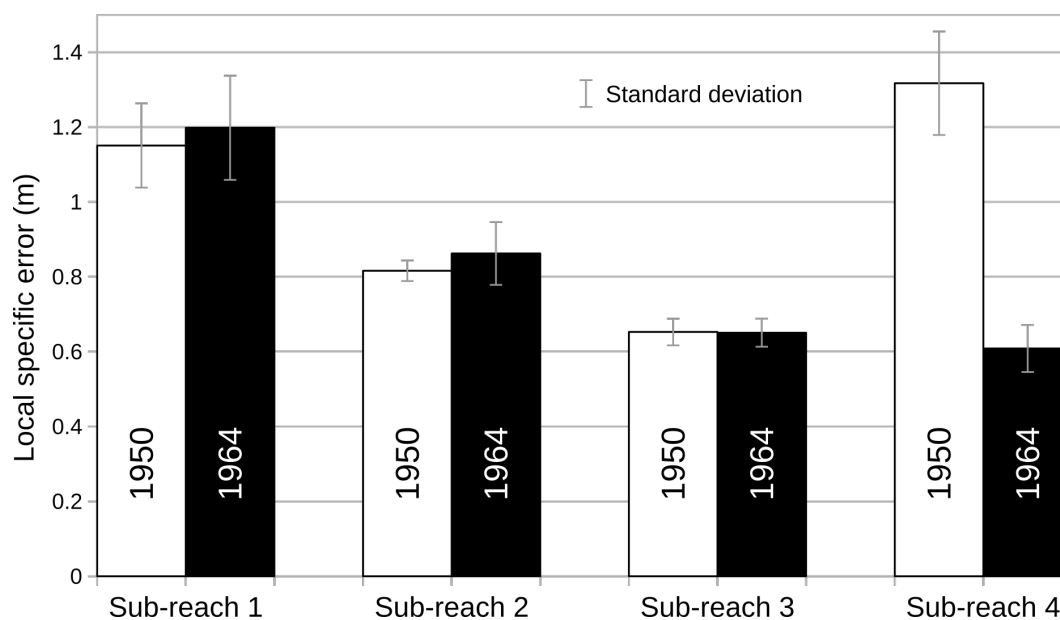
Figure 3. The independent set of GCPs used to assess SV-error on the study area. Background corresponds to a Sky View Factor visualisation of a 2015 LiDAR derived MNT.
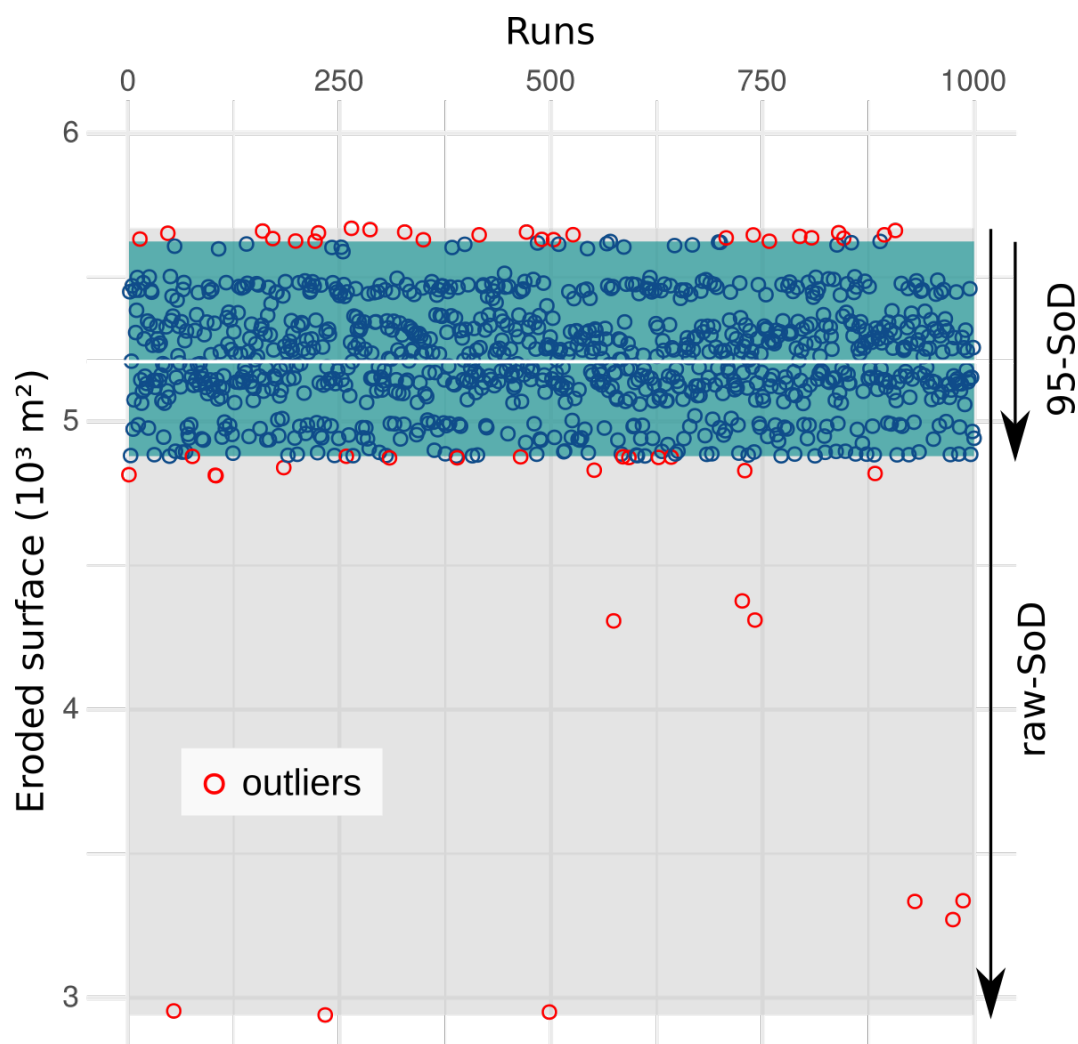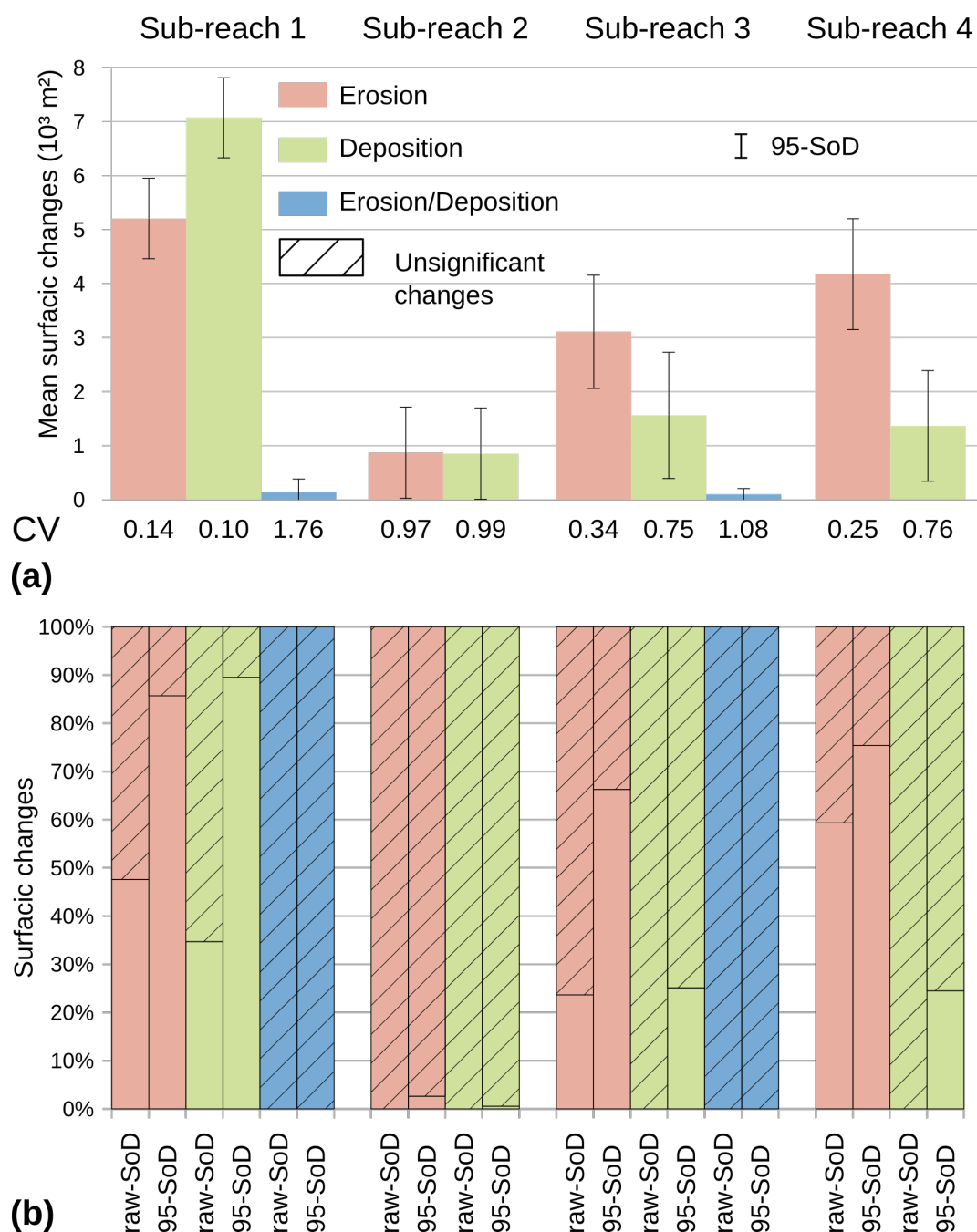
Figure 4. SV-error interpolation between GCPs from local RMSEs, by IDW method. Year 1950.
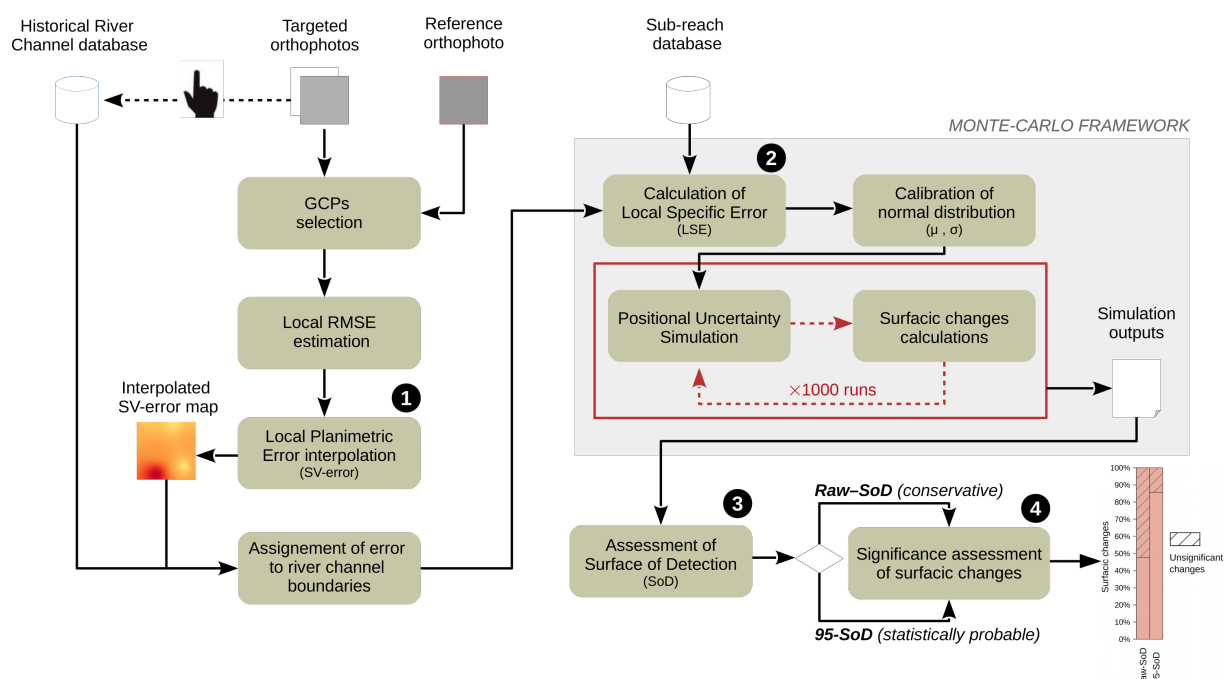
Figure 5. Local specific error calculated for each sub-reach, on both dates.

Figure 6. Measurements of eroded surface in sub-reach 1, through 1000 MC simulations. Gray horizontal line corresponds to the mean value.

Figure 7. (a) Mean surfacic changes and associated values of 95-SoD, for each sub-reach through Monte-Carlo simulation. CV: Coefficient of variation equal to the ratio 95-SoD/mean measured changes. (b) Significance of surfacic changes measurements when applying raw-SoD or 95-SoD.

Figure 8. Detailed flow chart of the methodology applied in this study, allowing to assess significance of eroded and/or deposited surfaces using SV-error.